Superconducting Single Photon Detectors Array Based on Hot Electron Phenomena

S. Ryabchun, A. Korneev, V. Matvienko, K. Smirnov, P. Kouminov, V. Seleznev, N. Kaurova, B. Voronov, G.N.Gol'tsman
Moscow State Pedagogical University, Malaya Pirogovskaya 1, Moscow, 11992, Russia
S. Polonsky
Picosecond Imaging Circuit Analysis, Optical Communications and High Speed Test, IBM T.J. Watson Research Centre

Abstract

In this paper we propose to use time domain multiplexing for large format arrays of superconducting single photon detectors (SSPDs) of the terahertz, visible and infrared frequency ranges based on ultrathin superconducting NbN films. Effective realization of time domain multiplexing for SSPD arrays is possible due to a short electric pulse of the SSPD as response to radiation quantum absorption, picosecond jitter and extremely low noise equivalent power (NEP). We present experimental results of testing 2×2 arrays in the infrared waveband. The measured noise equivalent power in the infrared and expected for the terahertz waveband is 10^{-21} $WHz^{-1/2}$. The best quantum efficiency (QE) of SSPD is 50% at 1.3 μm wavelength.

Introduction

Radioastronomy missions require detectors, which provide ultimate (background limited) sensitivity in the submillimeter wavelength range even when exposed to relatively weak background radiation. Several research groups are currently developing low noise superconducting detectors – both integrating direct detectors [1, 2] and quantum counting detectors [3, 4] – for terahertz range. Direct and quantum counting detectors have different detection mechanisms. In continuous integrating detectors energy of a large number of absorbed photons is distributed among a far larger number of elementary thermal excitations. Thus individual photons can not be distinguished. The response is effectively integrated over the response time of the detector. The number of excitations measures average radiation power that the detector absorbs. In a quantum, or photon, detector one photon creates excitations, which are collected and counted before they relax and before another photon is absorbed. Thus, each absorbed photon is registered. The number of collected excitations measures the energy of absorbed photon. These detectors can be compared in terms of Noise Equivalent Power (NEP). Integrating direct detectors can be of various types, for example, superconducting tunnel-junction detectors [5], or tungsten-based superconducting transition-edge sensors [6]. In this paper we present superconducting single photon detector (SSPD) potentially capable of operating in the infrared to terahertz waveband. The measured value of the SSPD NEP in the visible and infrared wavebands is $10^{-21}WHz^{-1/2}$.

Future submillimeter and far-infrared space telescopes will need large-format (of order of 10^3 elements) imaging detector arrays to perform astronomical observations. When the number of elements in array increases to order of thousand it becomes virtually impossible to realise an individual layout for every element. Various multiplexing systems were proposed; among them is one where elements are coupled with resonant circuits with different natural frequencies and multiplexing is realised by frequency dividing a signal [7]. Another approach [8] uses a frequency domain multiplexing scheme of the bolometer array. The bolometers are biased with ac currents whose frequencies are individual for each element and are much higher than the bolometer bandwidth. In another variant each detector is individually biased by dc of alternate polarities [9].

In this paper we present time domain multiplexing for SSPD arrays with all the detectors connected in series. Multiplexing is realised by comparing time delays between pulses coming from the opposite ends of an array. It should be noted that short response time of the SSPD (~200 ps [10]), low dark counts rate (less than 1 s^{-1}) [11], planar layout and relatively simple SSPD fabrication technology favour the integration of single detectors into an array with subsequent time domain multiplexing.

SSPDs photon-detection mechanism

For a detailed treatment of single photon detection we refer to [12, 13], here we only give a brief outline of the mechanism involved in the process. The mechanism of single photon detection by thin superconducting films biased close to the critical current of the film consists in the formation of the hot spot in the place of photon absorption resulting in voltage pulse generation which can be easily measured.

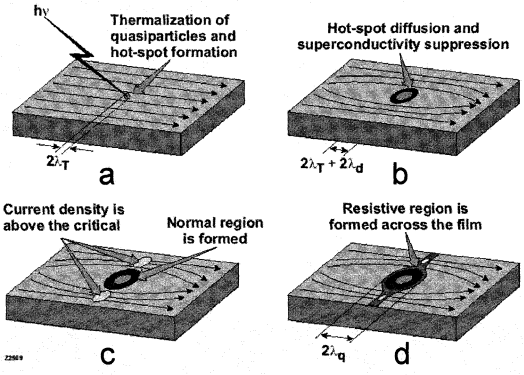

Fig. 1. Schematics of a hotspot-generated and supercurrent-assisted formation of a resistive barrier in an ultrathin and submicrometer-width superconducting stripe, kept at temperature far below T_c. The arrows indicate the flow direction of a supercurrent biasing the stripe.

SSPD consists of a superconducting stripe of a submicrometer width (comparable with the hotspot size) whose thickness is less than the electron thermalization length. The device is maintained at a temperature much lower than that of superconducting transition T_c and biased close to the device critical current I_c. The photoresponse mechanism is presented in Fig. 1. The collective action of the hotspot formation and I_b redistribution results in the appearance of the macroscopic resistive barrier across the SSPD stripe [12, 13]. As is illustrated in Fig. 1, after the localized hotspot is created [Fig. 1(a)], it then grows as quasiparticles diffuse out of the hotspot core. Simultaneously, the biasing supercurrent I_b is expelled from the resistive hotspot volume and concentrated in the "sidewalks" near the edges of the film [Fig. 1(b)]. Thus, I_b exceeds the critical value outside the hotspot, and phase-slip centres are created in quasi-one-dimensional sidewalks [Fig. 1(c)]. As a result, the superconductivity is destroyed, and a resistive barrier is formed across the entire cross-section of the stripe [Fig. 1(d)]. The resistive barrier gives rise to a voltage signal with the amplitude proportional to I_b. After its growth phase, the hotspot decreases due to the relaxation and out-diffusion of quasiparticles. Thus, after the quasiparticle relaxation time the hotspot in the stripe collapses, superconductivity (a zero resistance state) is restored, and the detector is ready to register another photon. As is seen from the above discussion the operation frequency range of the detector is determined by the ratio of the quantum energy to the energy gap of a superconductor. Low energy photon can not produce concentration of unpaired electrons that sufficient for superconductivity suppression. Quantum efficiency turns to be larger in a superconducting material with a smaller transition temperature as the superconducting energy gap decreases with transition temperature decrease. Thus, the use of a material with a smaller transition temperature will shift the cut-off towards longer wavelength [14].

SSPD array time domain multiplexing

A short response time of the SSPD (~200 ps [10]), low dark counts rate (less than 1 s^{-1}) and a short jitter (~30 ps) allow not only developing detectors of wide frequency range but also integrating them into large arrays with subsequent multiplexing, specifically, recognizing the signal with a two-channel read-out system. Figure 2 presents the principle of the time domain multiplexing of an SSPD array. All the SSPDs in the array are connected in series with delay lines and thus form a 50 Ω transmission line (Fig. 2). At the moment of any detector response there are two simultaneous voltage pulses propagating along the transmission line in the opposite directions. Both ends of the transmission line are loaded by the input of amplifiers A1 and A2. Their outputs are connected to the S(et) and R(eset) inputs of an SR-trigger. The time intervals between the pulses coming to the S and R inputs are different for each detector as they depend on the electro-magnetic lengths difference between the detector and amplifiers A1and A2 which are determined by the delay lines. Multiplexing of SSPD array elements will be

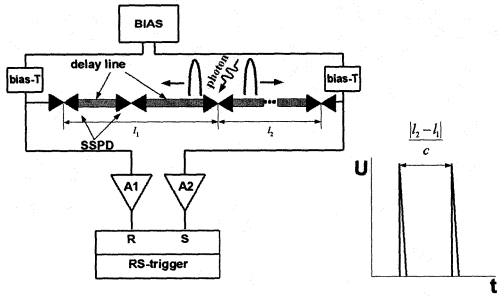

Fig.2. Time Domain Multiplexing of SSPD array

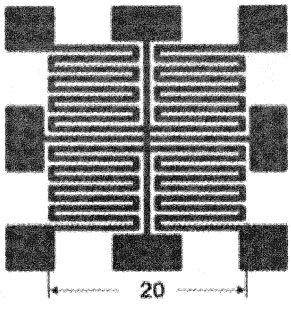

Fig.3. SSPD array layout. Active area – 4 pixels, pixel size - 10×10 μm^2, stripe width – 100 nm, thickness – 3.5 nm, filling factor – 0.5.

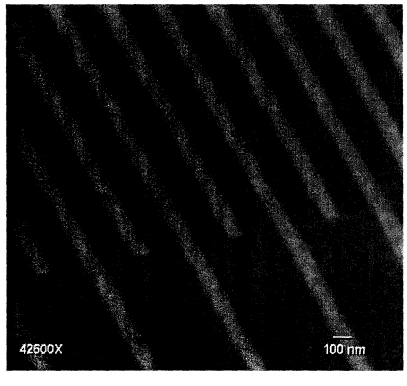

Fig. 4. Scanning electron microscope image of a small area of SSPD. 10×10 μm^2 3.5-nm-thick SSPD, the superconducting stripe width is ~100 nm.

realised by the determination of the pulse duration at the SR-trigger output. For successful time domain multiplexing of the system it is necessary the jitter be much shorter than delay times which eventually determine the rate of the array.

SSPD array fabrication

We manufactured SSPDs of the visible and infrared frequency ranges from 3.5-nm-thick NbN superconducting films, deposited on optical-quality sapphire substrates by dc reactive magnetron sputtering. The films are characterized by T_c = 10 to 11 K, superconducting transition width ΔT_c ~ 0.3 K, and critical current density j_c = 6 to 7×10^6 A/cm^2 at 4.2 K. Single devices are patterned into stripes with a nominal width of 80 to 100 nm. Our fabrication procedures, namely patterning based on the direct-electron-beam lithography, followed by reactive ion etching with a photoresist mask, are presented in detail in Ref. 15. To maximize the detector's active area, we have chosen a meander-type geometry with a device area of 10×10 μm^2 and a filling factor (the ratio of the active meander area to the nominal detector area) of up to 0.5. Thus, the total meander length is ~500 μm. Considering that for successful detector operation it is critical the superconducting stripe be uniform (effective deviation from the mean stripe width throughout the whole length should be such as to ensure uniform bias current density), manufacturing even single detector is not too easy a technological task. By the effective width of the stripe we understand not only its geometry but also its discontinuity which is determined by the raw superconducting film. When several detectors are integrated into an array the uniformity requirement holds true for all the detectors of the array.

To gain experience in the array fabrication technology and study time domain multiplexing capabilities we chose one of the simplest variants – a 2×2 array (fig. 3). Four elements (with a 10×10 μm^2 active area and a filling factor of 0.5) have a common ground contact. The other electrode between the two ground contacts is made so as to couple the matrix with a coplanar line. The layout also allows connecting the detectors in series in pairs as well as parallel connection. Figure 4 presents a micrograph of our 3.5-nm-thick SSPD with a filling factor of 0.5 etched in an interdigitated manner.

SSPD performance

As the uniformity of a meander is critical for optimal operation of our devices, we measured the

Table 1. SSPD 2×2 array characteristics: R_{300} – room temperature resistance, I_c – critical current at 2 K, QE – quantum efficiency of SSPDs at 2 K for 1.3 μm.

#	R_{300}, MOhm	I_c, $\times 10^{-6}$ A	QE, %
1	0.95	14.3	10
2	1.05	14.5	12
3	1.1	14.0	9
4	1.2	13.9	16

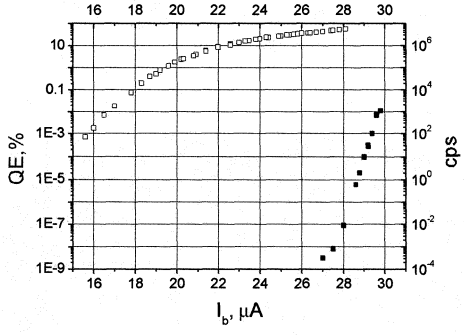

Fig. 5. Single SSPD quantum efficiency (open squares) and dark counts rate (solid squares) versus bias current at 2 K.

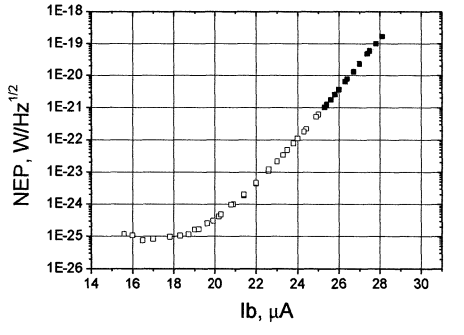

Fig. 6. Single SSPD NEP versus bias current 2 K – squares. The solid are measured data, the open are extrapolated date.

main parameters of our samples in an array, specifically, the room temperature resistance and critical current density. The values of these parameters for a 2×2 array are presented in table 1 where the first column shows the detector ordinal number. The 5 % spread in values of the samples characteristics at the constant current took place for other arrays as well and meets the time domain multiplexing requirements.

Another important characteristic of the SSPD is its quantum efficiency. Quantum efficiency (QE) is defined as the ratio of the number of photons registered by the detector to the number of photons incident on it. Figure 5 presents the quantum efficiency of the best single SSPD versus the bias current (I_b) for 1.3 μm wavelength at 2 K operating temperature. As radiation sources we used a continuous-wave laser diode. The same figure shows dark counts rate (R) dependence on the bias current at 2 K. As is seen from figure 5 the R versus I_b dependence obeys exponential law. For QE versus I_b dependence the slope decreases with I_b increase and for I_b close to I_c the dip of the QE curve is relatively slow. In the vicinity of the critical current QE goes up to ~50 %. We also measured QE of each detector of a 2×2 matrix for 1.3 μm wavelength at temperature 2 K. Table 1 shows the results of the measurement - all the four elements have high and almost equal quantum efficiency about 10%. The results obtained are important not in terms of high but in terms of equal values of QE of all the SSPDs in the array.

For comparison of direct and quantum counting detectors noise equivalent power (NEP) is introduced. The photon-counting process brings some peculiarities into signal processing. Because there is no integration time for a photon counter, a direct comparison of integrating detectors and quantum detectors in terms of their noise equivalent power is not possible. However, for quantum devices a parameter equivalent to NEP can be introduced as:

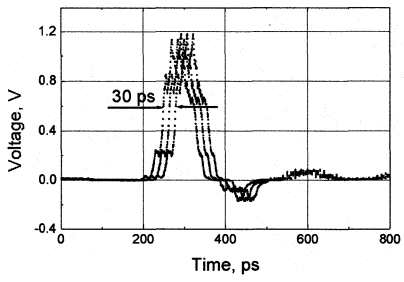

Fig. 7. SSPD jitter.

$$NEP = \frac{h\nu}{QE}\sqrt{2R} \qquad (1)$$

Figure 6 presents NEP versus I_b obtained using Eq. (1) and the experimental results for both QE and R presented in Fig. 6 for 2 K. The best achieved NEP value is of the order of 10^{-21} W/Hz$^{1/2}$ for 1.3 μm at 2 K. To our knowledge, this is the best sensitivity in the near-IR range ever reported for a single-photon detector. As we can see in fig. 6 the NEP rapidly decreases with the bias decrease, since close to I_c, R is a much stronger function of I_b than QE. The measured NEP is limited not by the detector properties but the measurement technique – integration time. The extrapolated values of dark counts rate lead to NEP values that reach 10^{-25} W/Hz$^{1/2}$ for 1.3 μm at 2 K.

We also measured one of the time characteristics of the SSPD – the jitter. The array time domain multiplexing will be restricted by SSPD jitter as it will set the lower limit of delay lines length between the elements of an array and thus determine the rate of the whole system. Figure 7 shows a time-resolved response pulse from our SSPD. The transient was taken at incident flux of about 10^3 photons per pulse with a bias current density of $0.6j_c$ and the oscilloscope working in the accumulation mode. The total system jitter was found to be about 30 ps. The value of the jitter includes the jitters of the laser system (20 ps), the output circuit and the oscilloscope (20 ps). Thus, the intrinsic SSPD jitter should be much less than 30 ps.

5. Conclusion

The method of array multiplexing presented in the paper can be realised for hot-electron single photon detectors of the visible, infrared and terahertz wavebands. This method enables us to develop an array detecting system outperforming a single SSPD in terms of 2D area scanning speed, which is certainly an advantage in the terahertz waveband or for large integrated circuits analysis.

The manufactured 2×2 SSPD array of the infrared waveband based on thin NbN superconducting film meets all the requirements of the time domain multiplexing. The characteristics of the best SSPD are the following: QE~50%, jitter < 30 ps, NEP ~ 10^{-21} WHz$^{-1/2}$. Increasing integration time determined by low dark counts rate will enable us in principle to reach SSPD noise equivalent power ~ 10^{-25} WHz$^{-1/2}$.

References

1. D. Chouvaev, L. Kuzmin, M. Tarasov, *Supercond. Sci. Technol.* **12**, 985, 1999.

2. B.S. Karasik, W.R. MacGrath, M.E. Gershenson, and A.V. Sergeev, *J. Appl. Phys.* **87**, 7586, 2000.

3. R.J. Schoelkopf, S.H. Moseley, C.M. Stahle, P. Wahlgren, and P. Delsing, *IEEE Trans. Appl. Supercond.* **9**, 2935, 1999.

4. S. Komiyama, O. Astafiev, V. Antonov, T. Kutsuwa, *Microelectronic Engineering*, **63**, 173-178, 2002.

5. de Bruijne, J. H. J., Reynolds, A. P., Perryman, M. A. C., Favata, F., and Peacock,A., 2002, *Opt. Eng.*, **41**, 1158–1169.

6. Cabrera, B., Clarke, R. M., Colling, P., Miller, A. J., Nam, S., and Romani, R. W., *Appl. Phys. Lett.*, **73**, 735–737, 1998; Miller, A. J., Nam, S. W., Martinis, J. M.,and Sergienko, A. V., *Appl. Phys. Lett.*, **83**, 791–793, 2003.

7. P.K. Day, H.G. LeDuc, B.A. Mazin, A. Vayonakis, J. Zmuidzinas, *Nature*, **425**, 817-821, 2003.

8. J. Yoon, J. Clarke, J.M. Gildemeister, A.T. Lee, M.J. Myers, P.L. Richards, and J.T. Skidmore, *Appl. Phys. Lett.* **78.** 371 (2001).

9. B. Karasik and William R. McGrath, *Proc. 12th Int. Symp. on Space Terahertz Technol.*, 436- 446, 2001.

10. Roman Sobolewski, A. Verevkin, G. N. Gol'tsman, A. Lipatov, and K. Wilsher, *IEEE Trans. Appl. Supercond.*,**13**, 1151-1157, 2003.

11. A. Verevkin, J. Zhang, W. Slysz, R. Sobolewski, A. Lipatov, O. Okunev, G. Chulkova, A. Korneev, K. Smirnov, G. Gol'tsman, A. Semenov, Proc. 13th Int. Symp. on Space Terahertz Technol., 105-112, 2002.

12. G.N. Gol'tsman, O. Okunev, G. Chulkova, A. Lipatov, A. Semenov, K. Smirnov, B. Voronov, A. Dzardanov, C. Williams, and Roman Sobolewski, *Appl. Phys. Lett.*, **79**, 705–707, 2001.

13. A.D. Semenov, G.N. Gol'tsman, and A. Korneev, *Physica C* **351**, 349, 2001.

14. G. Gol'tsman, A. Semenov, K. Smirnov, B.Voronov, Proc. 12th Int. Symp. on Space Terahertz Technol., 469-475, 2001

15. G.N. Gol'tsman, K. Smirnov, P. Kouminov, B. Voronov, N. Kaurova, V. Drakinsky, J. Zhang, A. Verevkin, and R. Sobolewski, *IEEE Trans. Appl. Supercond.*, 13, 192–195, 2003.